Resistance welding of TiNi-shape memory alloys

J.Beyer, E.J.M.Hiensch, University Twente, Department of Mechanical Engineering, Laboratory for Materials Science, Enschede, N.L.
P.A.Besselink, Foundation for Advanced Metals Science, (SGM) Hengelo, N.L.

Introduction

Joining processes as electronbeam welding, MIG-welding or laserbeam welding, where the joint is produced by melting of the material, are not suitable for shape memory TiNi-alloys due to the embrittlement of the welded region (1). Resistance butt-welding, especially of wires, has now been recognised as an effective process for joining SMA-parts, while preserving the SMA properties in the welded region (2,3). However, large scatter of the resulting properties has been obtained in case the welding conditions are not controlled within narrow limits. Important variables are: heat input, compression force, alignment and shape of the contact surface of the wires (flat or pointed).
A critical review of the welding process described in the previous paper (3) initiated the design and development of an improved welding instrument (4). An effort has been made to expand the practical utility of this process to a variety of wire diameters. The possibility of welding rings has been considered as a consequence of their large applicability.
This paper reports the further development and results obtained by this improved experimental setup.

Experimental

A Ti-50.3 at.% Ni shape memory alloy with a diameter of 5.6 mm., as supplied by Krupp, has been taken as the starting material (As-temperature of 313 K). The material was cold drawn to a variety of diameters (1.92, 1.43, 1.01, 0.49, 0.19 mm). After every reduction of area of 25 - 30%, the material was annealed at 923 K, except for the last memory heat treatment, which was taken as 773 K for 5 minutes. From each diameter, pieces of 15 mm. length were taken for the welding experiments; from the wires with a diameter of 1.92 and 1.43 mm, one end was conically ground with an apex angle of 90-100 degrees. The contact area during welding was thereby 40% of the wire cross section for these diameters. The thinner wires, down to 0.19 mm, were welded with flat perpendicular surfaces.
Determination of the transformation behaviour of base and weld material was carried out on a Stanton Redcroft DSC instrument. Tensile testing was carried out in a 20 kN tensile machine with a speed of 10 mm/min. Optical and electron microscopy (Jeol 200CX analytical TEM) were used to characterise the structural changes. TEM-specimens were prepared in a jet polishing machine containing a 7% solution of perchloric acid in methanol, at 285 K and 25 V.
The welding instrument has been described in a previous paper (3). The working principal is as follows. A compressive force is exerted on the ends of two wires, fixed into one movable and one fixed clamp. A current, supplied by a DC power regulator, is led into the wires, thereby heating the contact area. The compressive force will press the weak material outward, thus making a sound weld.
The following improvements have been made:
- a more rigid construction in order to make the alignment more accurate and reproducable, which now occurs with an optical microscope
- a whole set of clamping plates, one for each diameter (straight and rings).
- the compressive force, exerted on the two parts to be welded, is made

effectively constant during the welding cycle by using sets of disc-springs, instead of a single spring.
In order to weld a larger variety of wire diameters, a DC power supply of Weld Equip with a max. output of 3600 A was used. Fig. 1a represents the complete set-up and fig. 1b is a detail of the clamps with an as-welded ring.

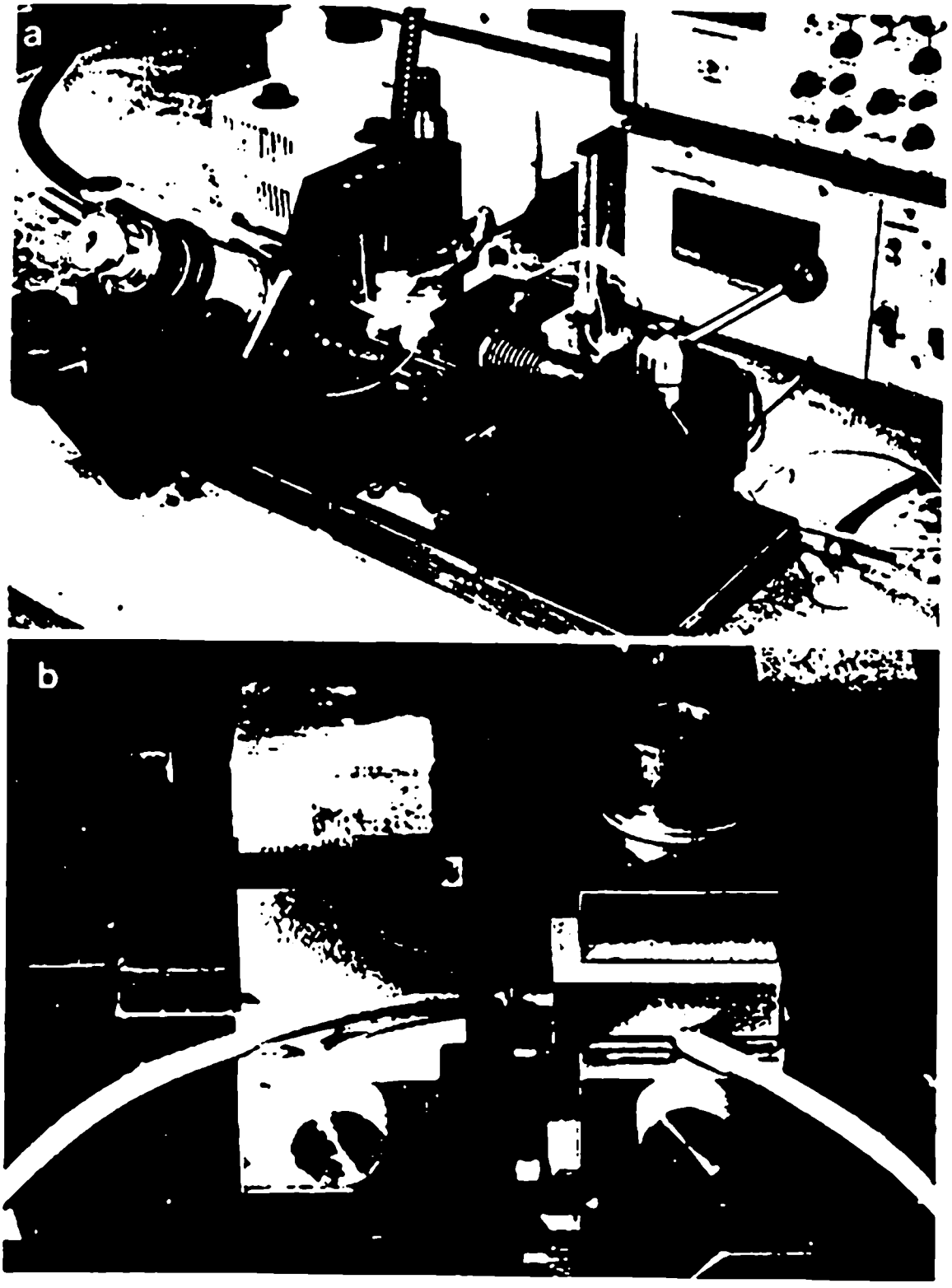

Fig. 1.
a: An overview of the present welding instrument.
b: Detail of the clamping system with an as-welded ring (wire diameter 2 mm).

Results and discussion

The optimum welding conditions, with respect to tensile strength, have been determined for each wire diameter. As an example, fig. 2 illustrates that there is a maximum tensile stress attainable for each series of compressive force exerted on the two parts to be welded.

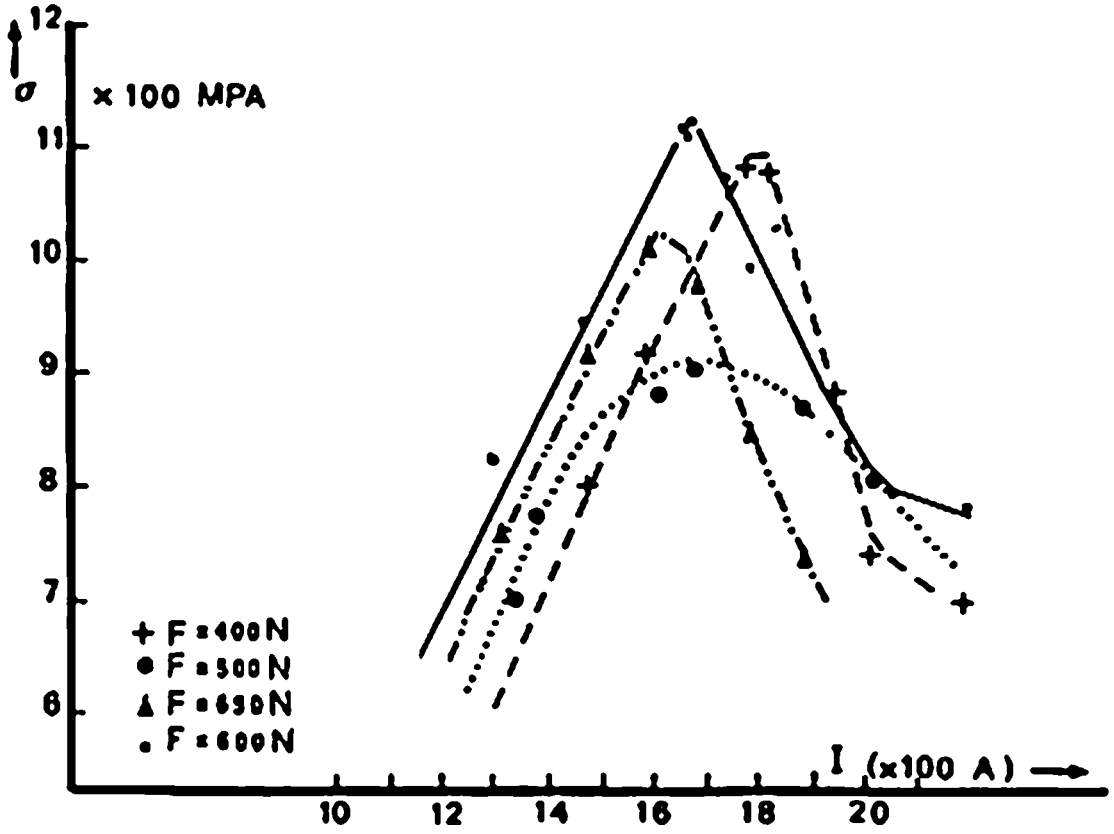

Fig. 2.
Tensile stress as a function of welding current for different compressive forces during welding.

The lower strength at higher currents indicate fracture outside the weld, due to excessive heating at the clamps. Table 1 summarizes the maximum attainable tensile stresses relative to the tensile stress of the base material. The recoverable strain which has been measured by a bending test with a maximum strain on the circumference of the wire of 6%, is also given.

Table 1.

Diameter (mm)	1.92	1.43	1.01	0.49	0.19
σ: % of max. tensile stress	85	93	97	97	100
shape recovery (%)	97-100	97-100	97-100	100	100

These relative values are noticably higher than the previously reported ones (70-80%). Relatively lower strength levels of the larger diameter wires are observed.
An explanation can be found in the conduction of the current from the clamps into the wire surface: as the wire diameter increases the current density at the surface will increase; the temperature at the surface is thus raised during welding. As a result, the structure will be weakened and failure outside the weld will occur on tensile testing.
For thicker wires a reconsideration of the clamping mechanism will be necessary. In addition, to minimise the electrical resistance between clamps and wire, eventually leading to hot spots, it is necessary to remove the oxyde layer.
It is important to notice, that the spread in the measured values was reduced to no more than 6%. This is mainly due to the better alignment possibilities, resulting in better parallelism of the wire contact surfaces.
In order to obtain a proper weld, the Heat Input (HI) J/mm^2 during the welding period ($t_1 + t_2 + t_3$) showed to be a dominant factor.

$$HI = I^2(t).R.dt \qquad \text{and} \qquad R = U/I$$

where U = welding voltage and I = max.current (at t_2) when U is reached.

A linear relationship between HI and different diameters, as indicated in fig. 3, is found for the wires up to 1 mm diameter, where a flat contact surface is used. The relationship only accounts for the initial length of the wire between the movable clamps.

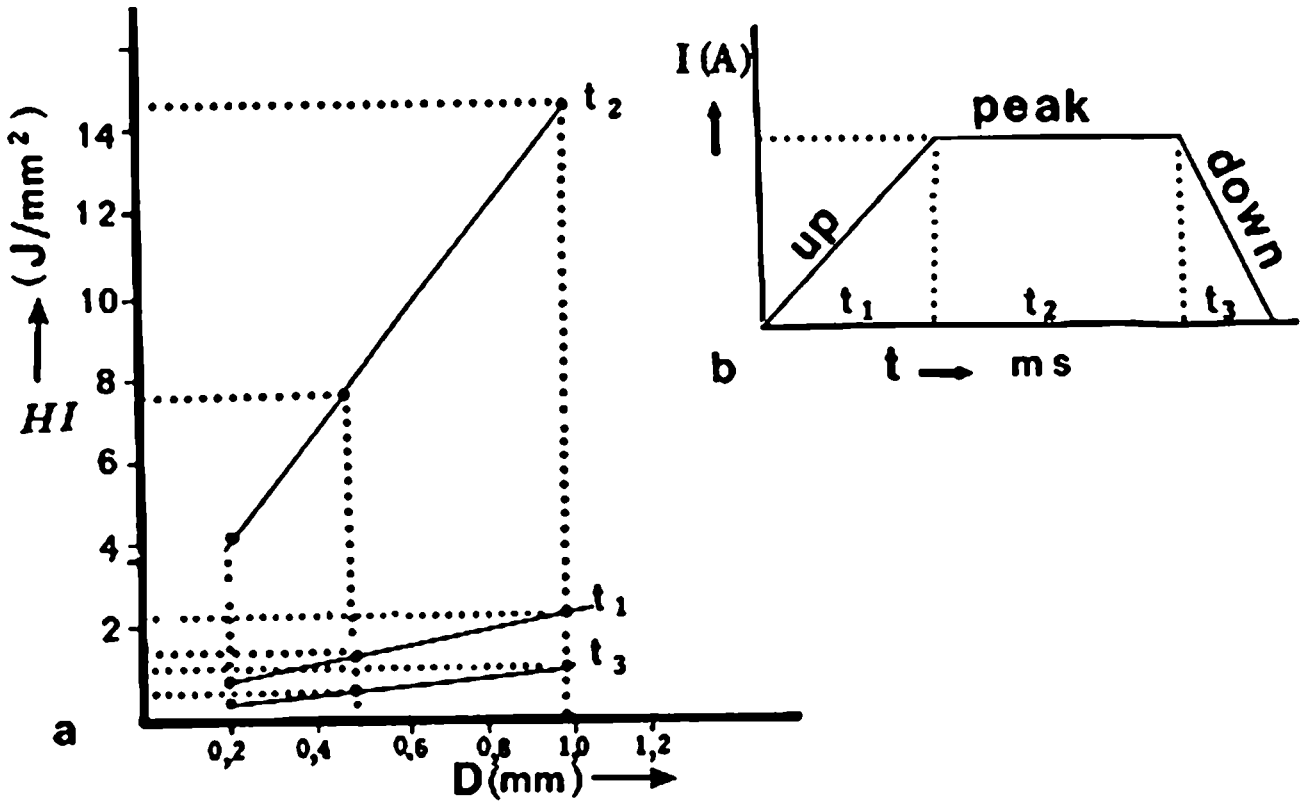

Fig. 3.
a: Relation between heat input and wire diameter.
b: The welding current is build up in 3 periods during welding.

The heat losses through the clamps and the change of l during welding are not considered. Experiments show, that if the change of length is limited, which can be done by variation of the welding time ($t_1 + t_2 + t_3$) using the same heat input, the tensile stress of the weld can raise to a value even closer to that of the base material as indicated in table 1. The deviation of the calculated HI and the actual one for the results reported, showed to be within 8% at present. The applied compressive stress and the current density can be calculated from the empirical relation

$$\sigma(d_1)=\sigma(d_2).(d_1/d_2)^{\frac{1}{2}} \quad \text{and} \quad J(d_1)=J(d_2).(d_1/d_2)^{\frac{1}{2}}$$

Although more data are required to be conclusive, the same type of behaviour is proposed for the larger diameter wires with conical shaped edges. Rings of the same material (ring diameter 21 mm) are also welded with the use of the same parameters. The same tensile strengths were obtained as reported for the straight wires (diameter 2 mm).
The promising results of the tensile tests alone, are no guarantee for good fatigue properties. DSC measurements were carried out to elucidate the transformation behaviour of the weld relative to the base material.
Fig. 4 shows a DSC curve for the weld as well as for the base (2 mm) wire. The heating and the cooling part of the curves have to be considered separately. On heating, the martensite - austenite transformation occurs at the same temperature. This is important, because the SMA effect occurs in this region. On cooling it can be noted, that the weld and the base material behave differently. The base material first transforms to R-phase (T_R is 333 K) and the martensite is well separated from the R-phase with an Ms-temperature of 271 K. The weld metal has a Ms-temperature of 285 K. These appreciable differences in transformation temperatures will lead to a build up of tensile stresses, either in the welded region or in the base material, depending on the relative position of the curves.

x

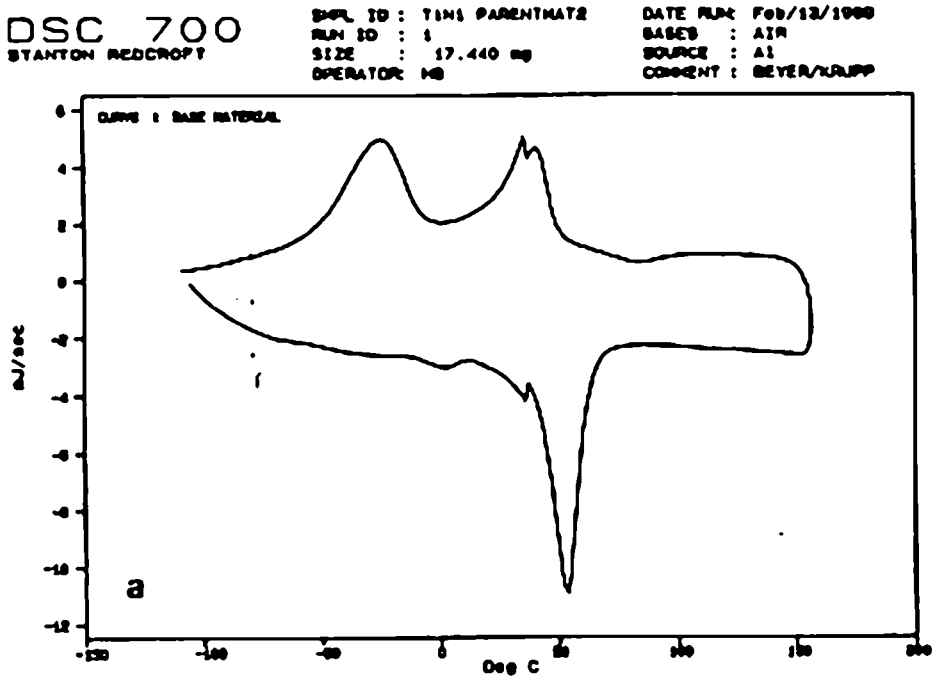

x

x

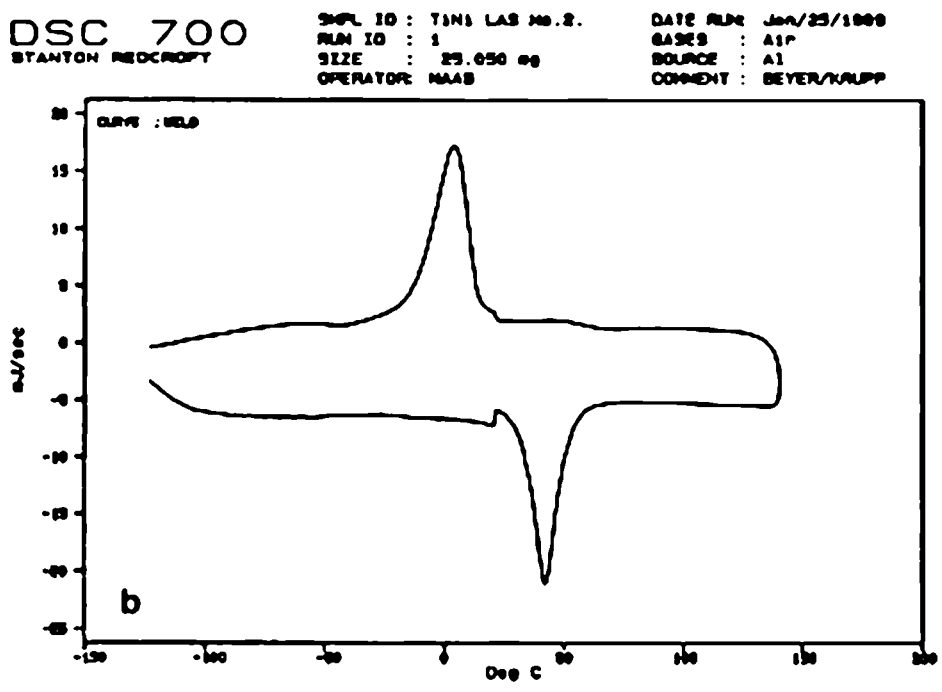

x

Fig. 4.
DSC-curves for the base material (a) and the weld (b).

Successive transformation cycles can initiate early failure in the vicinity of the weld. This can than lead to the deterioration of the fatigue properties, while the SMA-part is in service. The DSC curve also indicates the lowest temperature (Mf) to which the material should be cooled in practice. The weld and base material should be fully martensitic before straining in order to obtain repeated SMA-behaviour.
The optical and electron micrographs of fig. 5 show the microstructure of the weld and the base material.

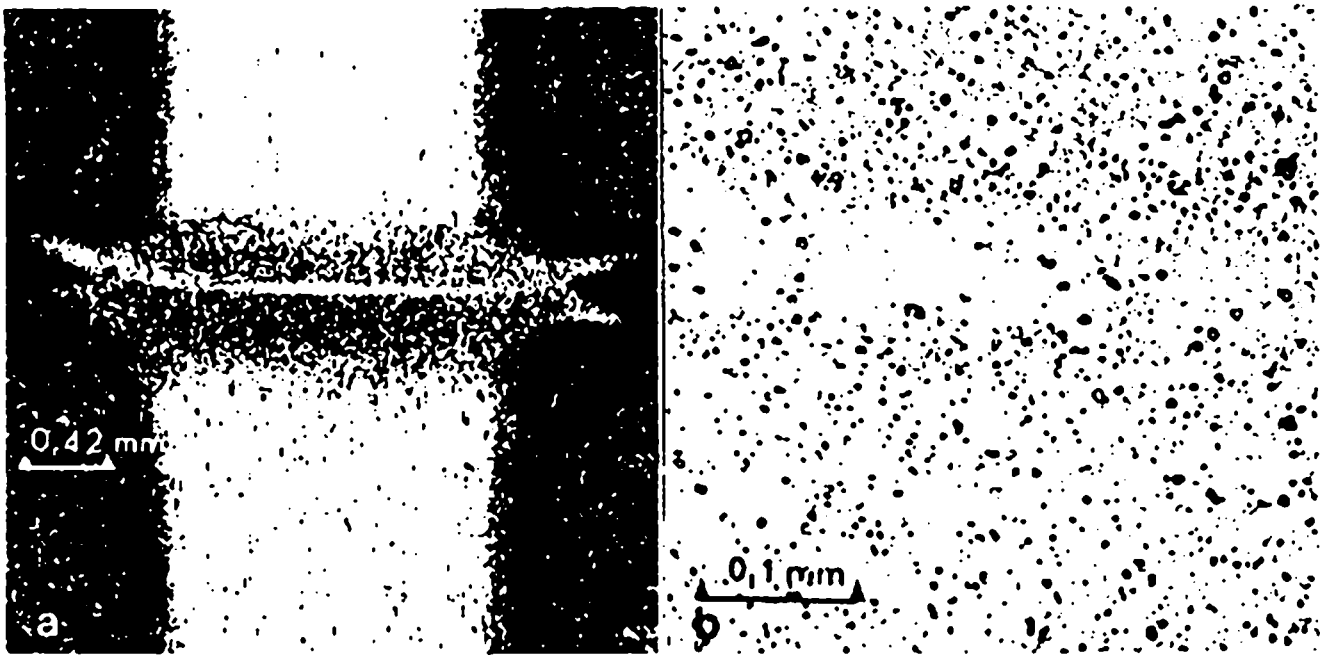

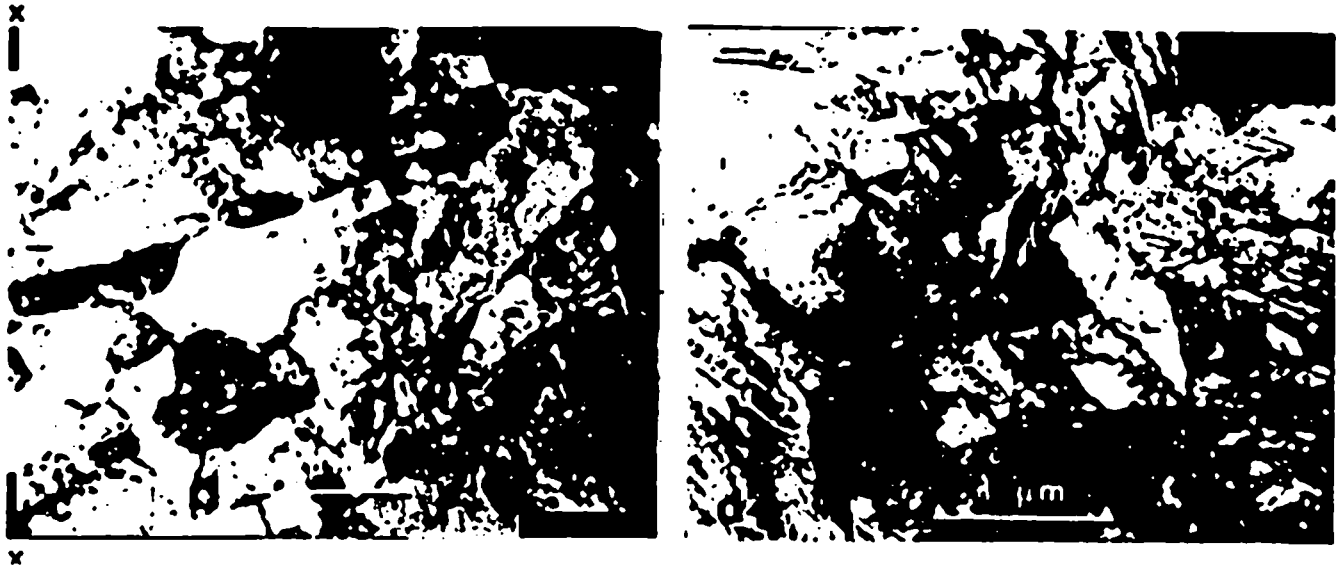

Fig. 5.
a: Cross section of a 2 mm welded wire.
b: Microstructure of the weld.
c: TEM micrograph of the austenitic base material.
d: TEM micrograph of the martensitic weld

The welded region in the optical micrograph is approximately 0.2 mm wide. The grain size in the weld is about 2 times smaller than in the base material. The weld itself seems to have less Ti_2Ni particles than the heat affected zone, as was described previously (3).
The electron micrographs show that the weld is transformed to martensite, whereas the base material is still austenitic. The electropolishing in this example is carried out at 283 K.
The DSC results show that this temperature is just between the two transformation regimes of the weld and the base material. On cooling this causes stresses resulting in the enhancement of the dislocation density.
These results show that apart from the tensile testing, which reflects the optimum welding conditions, it is important to characterise the transformation behaviour by DSC (or other physical techniques).

In order to test the usefulness of this welding technique, another alloy in the pseudo elastic condition has been welded. The first preliminary results indicate an even slightly better tensile strength in the welds: 93% for 1.92 mm wire and 97% for a 1.32 mm wire. It is speculated, that the electrical resistance of the B_2 phase is higher than for the martensite, which leads to lower current density and less variation in properties due to hot spots at the clamps.

Conclusions

The newly designed welding instrument showed to produce welds with SMA properties and behaviour which is comparable with that of the base material.
An empirical relation is found for the heat input and the wire diameter, which makes the determination of the proper experimental parameters simple in practice.
The applicability of this technique to straight and ring shaped material is demonstrated.
Welding of martensitic as well as austenitic TiNi-alloys in various shapes is

possible and will be demonstrated in the near future.
DSC measurements are a requirement, apart from mechanical testing, to specify the quality of the weld.

References

(1) C.M. Jackson, H.J. Wagner and R.J. Wasilewski, Nasa Report, SP 5110 (1972)
(2) N. Nishikawa, H. Tanaka, M. Kohda, T. Nagaura and K. Watanabe, Journal de Physique 43 (1982) C 4-839.
(3) J. Beyer, P.A. Besselink and J.H. Lindenhovius, Proc SMA 1986 Conference, Guilin, China, 492.
(4) N. van Leerdam, private communication, University Twente.